Asian Journal of Civil Engineering
https://doi.org/10.1007/s42107-023-00743-w

RESEARCH

GBRT-based model for predicting the axial load capacity of the CFS-SOHS columns

Duy-Duan Nguyen[1] · **Trong-Ha Nguyen**[1]

Received: 16 May 2023 / Accepted: 28 May 2023

Abstract
This study presented the performance of the gradient boosted regression trees (GBRT) model for predicting the axial load capacity (ALC) of the cold-formed steel semi-oval hollow section (CFS-SOHS) columns. A total of 219 datasets were carefully collected from previous publications including experimental and numerical results, which were used to develop the GBRT model. Of these, 209 datasets were used for training, while 10 datasets were used for testing. The results obtained from the GBRT model were compared with two existing formulas based on the statistical metrics (R^2, RMSE, and$a20-$ index). The statistical metrics from the GBRT model ($R^2 = 0.9999$, RMSE $= 29.458$, and $i20-$ index $= 1.000$) have been the best-predicting to the ALC of the CFS-SOHS column. Finally, a new graphical user interface (GUI) tool was built based on the regression model for practice design.

Keywords Semi-oval hollow section · Critical buckling load · Steel column · GBRT model · Machine learning

Introduction

Recently, the cold-formed steel semi-oval hollow section (CFS-SOHS) column has been widely used in civil and industrial steel buildings. Furthermore, CFS-SOHS columns have a higher compression capacity and aesthetics compared to square and circular cross-section columns (Zhu & Young, 2011, 2012). However, current design codes such as ANSI, AS/NZS, and Eurocode do not support this cross-section type, while previous publications have differences between numerical, theoretical, and experimental results. Thus, this has urged researchers to study theoretical, numerical, and experiments on the CFS-SOHS members (Chen & Young, 2018a, 2018b).

So far, machine-learning (ML) has been applied in many fields, such as engineering, economics, and social problems (Kaveh, 2014; Kaveh & Khavaninzadeh, 2023; Kaveh & Servati, 2001; Manna et al., 2017; Naser et al., 2021; Nguyen et al., 2021a; Nguyen et al., 2021b, 2022b; Nguyen et al., 2023; Qi et al., 2018; Tran et al., 2021; Tran & Kim, 2020; Tran et al., 2019). Meanwhile, the GBRT model emerged as a powerful regression tool. Particularly, it was used for prediction, analysis, and structural behaviors (Hao et al., 2022; Manna et al., 2017; Nieto et al., 2018; Prettenhofer & Louppe, 2014; Qi et al., 2018; Tran & Kim, 2022). The GBRT model was employed for predicting the behavior of concrete (Bakouregui et al., 2021; Dahiya et al., 2021; Shatnawi et al., 2022), and steel structures (Nguyen et al., 2022a; Nieto et al., 2018; Truong et al., 2020; Wang & Song, 2020). It can be seen that among many published studies, there were no studies used the GBRT model for predicting the ALC of the CFS-SOHS columns.

This study aims to propose a GBRT model for predicting the ALC of the CFS-SOHS columns. For that, 219 datasets were carefully collected from previous publications including experimental and numerical results. Of these, 209 datasets were used for training, while 10 datasets were used for testing. Also in this model, the overall depth (D), the overall width (B), thickness (t), and column length (L) are input parameters, while the ALC of the CFS-SOHS columns is an output parameter. The results obtained from the GBRT model were compared with two existing formulas. The statistical metrics (R^2, RMSE, and$a20-$ index) were used for the predictive performance assessment of the GBRT model.

✉ Trong-Ha Nguyen
trongha@vinhuni.edu.vn

Duy-Duan Nguyen
duan468@gmail.com

[1] Department of Civil Engineering, Vinh University, Vinh 461010, Vietnam

Published online: 18 June 2023

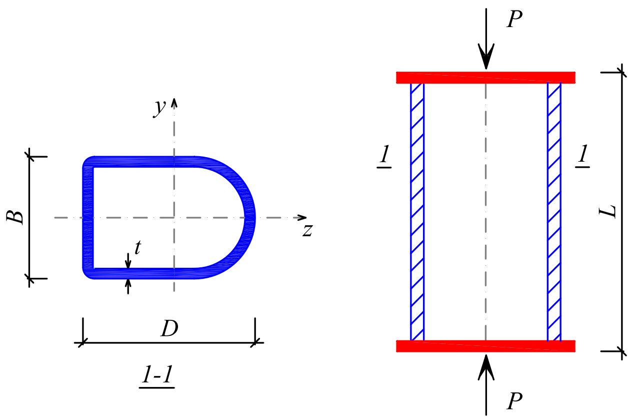

Fig. 1 The cold-formed steel SOHS column

Table 1 The range statistics properties of the database

Variable	D(mm) (X_1)	B(mm) (X_2)	t(mm) (X_3)	L(mm) (X_4)	P(kN) (output)
Minimum	93.00	60.00	2.00	200.00	176.00
Mean	301.51	174.88	7.13	2393.38	2681.80
Maximum	450.00	360.00	20.00	4000.00	14,231.20
SD	136.22	84.56	5.34	1115.52	3349.41
COV	0.45	0.48	0.75	0.47	1.25

Finally, a new graphical user interface (GUI) tool was built based on the regression model for practice design (Fig. 1).

Dataset collection

In machine learning models, the training datasets decided the performance of the models. This study used a set of 219 data carefully collected from previous publications including experimental and numerical results (Chen & Young, 2018a, 2018b), which were used to develop the GBRT model. The dataset has four input parameters including the overall depth (D), the overall width (B), thickness (t), and column length (L), while the ALC of the CFS-SOHS columns is an output parameter. The range, statistical properties, and histograms of the datasets are shown in Table 1 and Fig. 2.

Figure 3 shows the correlation matrix between the input and output parameters of the dataset. From this figure, it can be seen that the Pearson correlation coefficient has a maximum is 0.925, and a minimum is 0.062. In general, the Pearson correlation coefficient of the remaining parameters has a weak correlation. This can be confirmed that the dataset used to develop the GBRT model for predicting ALC of the CFS-SOHS columns was the scientific and practical significance.

Existing formulas for the ALC of the CFS-SOHS columns

To predictive performance assessment of the GBRT model, this study used two existing formulas, which have been proposed by Chen and Young (Chen & Young, 2018b), and standard codes AISI-S100-16 (AISI-S100, 2016). To the knowledge of the authors, two existing formulas that have predictive performance are the most effective (Table 2).

Gradient boosting regression tree (GBRT)

The GBRT is a machine-learning algorithm. It is a prediction algorithm based on a regression model that has been widely used in many fields (Friedman, 2001; Hao et al., 2022; Manna et al., 2017; Qi et al., 2018). The GBRT algorithm is a combination algorithm of the gradient boosting (GB) algorithm and regression tree (RT) algorithm. It was born to improve the limitations of the two algorithms above (Friedman, 2001).

The prediction technical of GBRT can be summarized in the following steps (Prettenhofer & Louppe, 2014).

1. An initial regression model is created;
2. The next regression tree is trained to take the residuals of the previous regression tree;
3. Through many iterations, finally obtain a model with high accuracy for prediction results.

The GBRT can be shown as the mathematical expression.

Considering loss function $L(y, F(x))$, input dataset $D =$, and output function value $F_K(x)$.

Algorithms

$$F_0(x) = \arg\min_{h(x)} \sum_{i=1}^{n} L\left(y_i, h(x)\right) \quad (3)$$

For $1 to K$

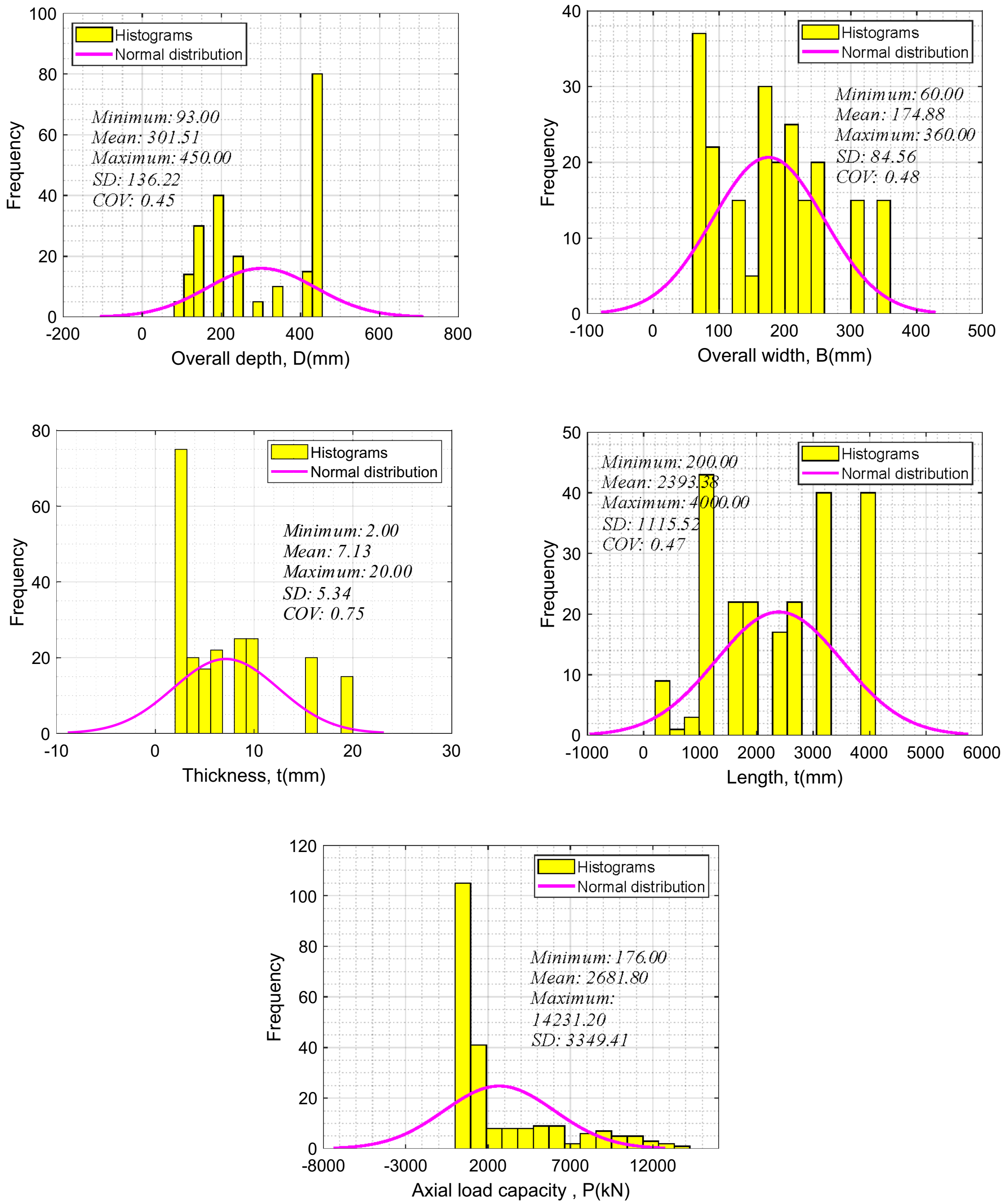

Fig. 2 Histogram of the dataset

	D	*B*	*t*	*L*	*P_test*
D	1.000	0.846	0.376	0.237	0.566
B	0.846	1.000	0.356	0.199	0.558
t	0.376	0.356	1.000	0.049	0.925
L	0.237	0.199	0.049	1.000	0.062
P_test	0.566	0.558	0.925	0.062	1.000

Fig. 3 Correlation matrix of the datasets

$$\gamma_k(x) = \underset{\gamma}{\operatorname{argmin}} \sum_{i=1}^{n} L\left(y_i, F_{k-1}(x_i) - \gamma \frac{\partial L(y_i, F_{k-1}(x_i))}{\partial F_{k-1}(x_i)}\right) \tag{4}$$

where

$$F_k(x) = F_{k-1}(x) - \gamma_k \sum_{i=1}^{n} \nabla_F (y_i, F_{k-1}(x_i)) \tag{5}$$

In where, $L(y_i, F(x))$ is loss function, D is training set, (x_1, y_1) the first set of data, K is the number of iterations, $F_K(x)$ is final model; F_k is the model after each iteration; $F_0(x)$ is initial model, $h(x)$ represents predictions generated by the model; γ_k is the weight of the k^{th} model. The implementation steps of the GBRT are shown in Fig. 4.

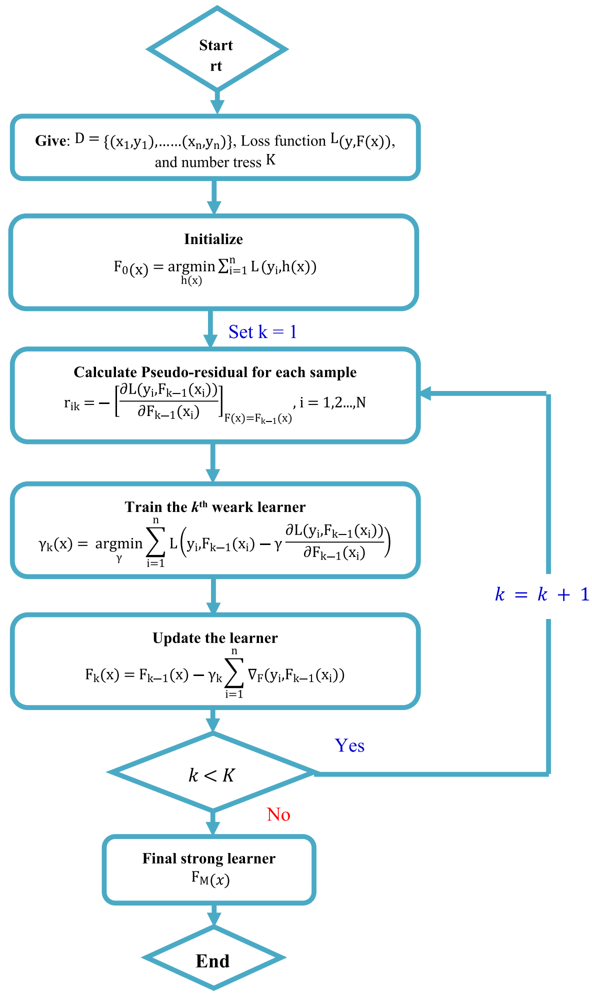

Fig. 4 Flowchart of the GBRT model

Development of the GBRT model

Input and output parameter, and GBRT model

To develop the GBRT model in this study, the overall depth (*D*), the overall width (*B*), thickness (*t*), and column length (*L*) are considered input parameters, while the ALC of the CFS-SOHS columns is an output parameter. The database is randomly split into six training–testing set 0.95–0.05 (GBRT-01), 0.90–0.10 (GBRT-02), 0.85–0.15 (GBRT-03), 0.80–0.20 (GBRT-04), 0.75–0.25 (GBRT-05), and 0.70–0.30 (GBRT-06). A GBRT model has the best-performing. If the indices, $a20-$index, R^2 has the greatest value, and RMSE has the smallest value. According to Zorlu et al. (Zorlu et al., 2008) the expressions for determining these indexes has the form.

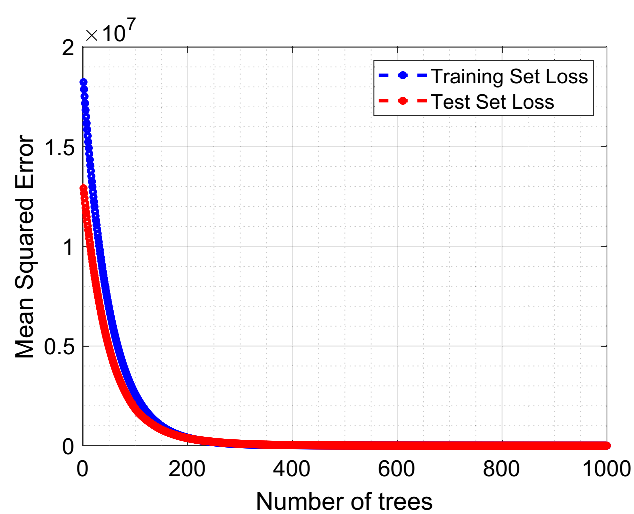

Fig. 5 The convergence curves of the GBRT-01 model

Table 2 Existing formulas for the ALC of the CFS-SOHS columns

References	Formulas
Chen et al. (Chen & Young, 2018b)	$\left(P^*_{\mathrm{DSM}}\right) = \min\left(P^*_{nl}, P^*_{ne}\right)$ (1) $P^*_{nl} = \begin{cases} 1.2P_y & \text{for } \lambda_l \le 0.472 \\ \left[1 - 0.168\left(\frac{P_{crl}}{P_y}\right)^{0.34}\right]\left(\frac{P_{crl}}{P_y}\right)^{0.34} P_y & \text{for } \lambda_l > 0.472 \end{cases}$ with $\lambda_l \le 0.702$ $K = 1.05 - 0.1\lambda_l; R = 2.5 - 0.025\lambda_l; Q = \left(\frac{0.21925}{K}\right)^{\frac{1}{2R}}$ $\lambda_l = \sqrt{\frac{P_y}{P_{crl}}}; \lambda_c = \sqrt{\frac{f_y}{f_{cre}}}; f_{cre} = \frac{\pi^2 E}{(L_e/r)^2}; P_y = f_y.A$ $P^*_{ne} = \begin{cases} \left(1.2 - 0.6\lambda_c\right)P_y & \text{for } \lambda_c \le 0.5 \\ \left(\frac{0.877}{\lambda_c^2}\right)P_y & \text{for } \lambda_c > 0.5 \end{cases}$ with $\lambda_l > 0.702$ $P^*_{ne} = \begin{cases} \left(KQ^{\lambda^R}\right)P^*_{nl} & \text{for } \lambda_c \le 2.0 \\ \left(\frac{0.877}{\lambda_c^2}\right)P_y & \text{for } \lambda_c > 2.0 \end{cases}$
AISI-S100-16 (AISI-S100, 2016)	$P^*_{\mathrm{DSM}} = P_{nl}$ (2) $P_{nl} = \begin{cases} P_{ne} & \text{for } \lambda_l \le 0.776 \\ \left[1 - 0.15\left(\frac{P_{crl}}{P_{ne}}\right)^{0.4}\right]\left(\frac{P_{crl}}{P_{ne}}\right)^{0.4} P_{ne} & \text{for } \lambda_l > 0.776 \end{cases}$ $\lambda_l = \sqrt{\frac{P_{ne}}{P_{\mathrm{crl}}}}; P_{ne} = A_g F_n$ $\lambda_c = \sqrt{\frac{F_y}{F_{\mathrm{cre}}}}; F_{\mathrm{cre}} = \frac{\pi^2 E}{(KL/r)^2}.P_{crl} = F_{\mathrm{crl}} A_g = K\frac{\pi^2 E}{12(1-\mu^2)}\left(\frac{t}{w}\right)^2$ $F_n = \begin{cases} \left(0.658^{\lambda^2}\right)F_y & \text{for } \lambda_c \le 1.50 \\ \left(\frac{0.877}{\lambda_c^2}\right)F_y & \text{for } \lambda_c > 1.50 \end{cases}$

$$R^2 = 1\left(\frac{\sum_{i=1}^{n}\left(t_i - o_i\right)^2}{\sum_{i=1}^{n} o_i^2}\right); \tag{6}$$

$$\mathrm{RMSE} = \sqrt{\left(\frac{1}{n}\right)\sum_{i=1}^{n}\left(t_i - o_i\right)^2}; \tag{7}$$

$$a20 - \text{index} = \frac{m20}{n}. \tag{8}$$

where t_i is the ith output parameter of collected data; o_i is the ith predicted value of GBRT model; n is the number of samples; $m20$ is the number of samples has a ratio of the output parameter and predicted value between the range $0.8 - 1.2$.

Table 3 is shown the ranking of the GBTR models based on the ($a20 -$ index, R^2, and RMSE). noting that the best value increments from 1 to 6. From this table, the GBRT-01 model (with a training–testing ratio is 0.95–0.05) has the highest ranking. Thus, this study uses the GBRT-01 model for predicting the ALC of the CFS-SOHS columns.

Performance of the GBRT-01 model

Figure 5 shows the convergence curves of the GBRT-01 model. It is best-performing at MSE = 3.12×10^{-6} after 1000 trees, it can be seen that the MSE value is close to zero. The results obtained confirm that the GBRT-01 model has predicted the ALC of the CFS-SOHS columns very well.

Figure 6 shows the regression between the actual and predicted value of the GBRT-01 model. The R^2 values for training data, testing data, and all data are 0.9999, 0.9997, and 0.9999, respectively.

Figure 7 shows the comparison between actual and predicted data of the ALC of the CFS-SOHS columns obtained

Table 3 The ranking of the GBRT models based on the ranking of the $a20-index$, R^2, and $RMSE$

Model	Ratio	Data sets	R^2	Rating for R^2	RMSE	Rating for RMSE	$a20-$ index	Rating for $a20-$ index	Rank value
GBRT-01	0.95	Training	1.000	6	29.458	6	1.000	5	17
	0.05	Testing	1.000	6	46.200	6	1.000	3	15
		All	1.000	6	30.424	6	1.000	5	17
Total rank									**49**
GBRT-02	0.90	Training	1.000	5	50.035	5	0.995	4	14
	0.10	Testing	0.999	5	115.281	5	1.000	3	13
		All	1.000	5	59.479	5	0.995	3	13
Total rank									**40**
GBRT-03	0.85	Training	1.000	4	62.164	4	0.995	2	10
	0.15	Testing	0.998	4	159.851	4	1.000	3	11
		All	0.999	4	83.865	4	0.995	3	11
Total rank									**32**
GBRT-04	0.80	Training	0.999	1	92.615	1	1.000	5	7
	0.20	Testing	0.998	3	179.664	3	1.000	3	9
		All	0.998	3	115.027	3	1.000	5	11
Total rank									**27**
GBRT-05	0.75	Training	0.999	2	85.779	2	0.995	2	6
	0.25	Testing	0.975	2	546.339	2	0.815	2	6
		All	0.993	2	281.324	2	0.941	2	6
Total rank									**18**
GBRT-06	0.70	Training	1.000	3	66.678	3	0.968	1	7
	0.30	Testing	0.970	1	600.083	1	0.708	1	3
		All	0.990	1	331.670	1	0.890	1	3
Total rank									**13**

Bold numbers highlight the total ranking of different GBRT models

Table 4 Performance of different predictive models

Predicted model	R^2	RMSE (kN)	$a20$ index	$P_{Prediction}/P_{test}$				
				Min	Max	Mean	StD	COV
Chen & Young	0.9894	407.605	0.8401	0.4664	1.2064	0.9303	0.1336	0.1436
S100-16	0.9125	1172.044	0.2329	0.5084	5.0405	1.7311	1.0753	0.6211
GBRT-01	**0.9999**	**29.458**	**1.0000**	**0.8550**	**1.1373**	**0.9997**	**0.0349**	**0.0349**

Bold numbers emphasize the calculated statistical values of the GBRT model

from the GBRT-01 model. Can be seen that the error between actual and predicted data was trivial. Once again affirmation the GBRT-01 has good performance and was highly reliable for the prediction of the ALC of the CFS-SOHS columns.

Results and discussions

To assert the superior prediction of the GBRT-01 model for the ALC of the CFS-SOHS columns. In this work, the results obtained from the GBRT-01 model were compared with two existing formulas, which were proposed by Chen et al. (Chen & Young, 2018b) and standard codes AISI-S100-16 (AISI-S100, 2016). Three statistical metrics (R^2, RMSE, and $a20-$ index) were used. Table 2 shows the results compared between the results obtained from the GBRT-01 model with two existing formulas. In this table, the R^2, RMSE, and $a20-$ index values of the GBRT-01 model and two existing formulas are (0.9999, 0.9894, 0.9125), (29.458, 407.605, 1172.044) kN, and (0.1000, 0.8401, 0.2329), respectively. Moreover, the statistical metrics such as minimum, mean, maximum, StD, and CoV obtained from the GBRT-01 model are much better than

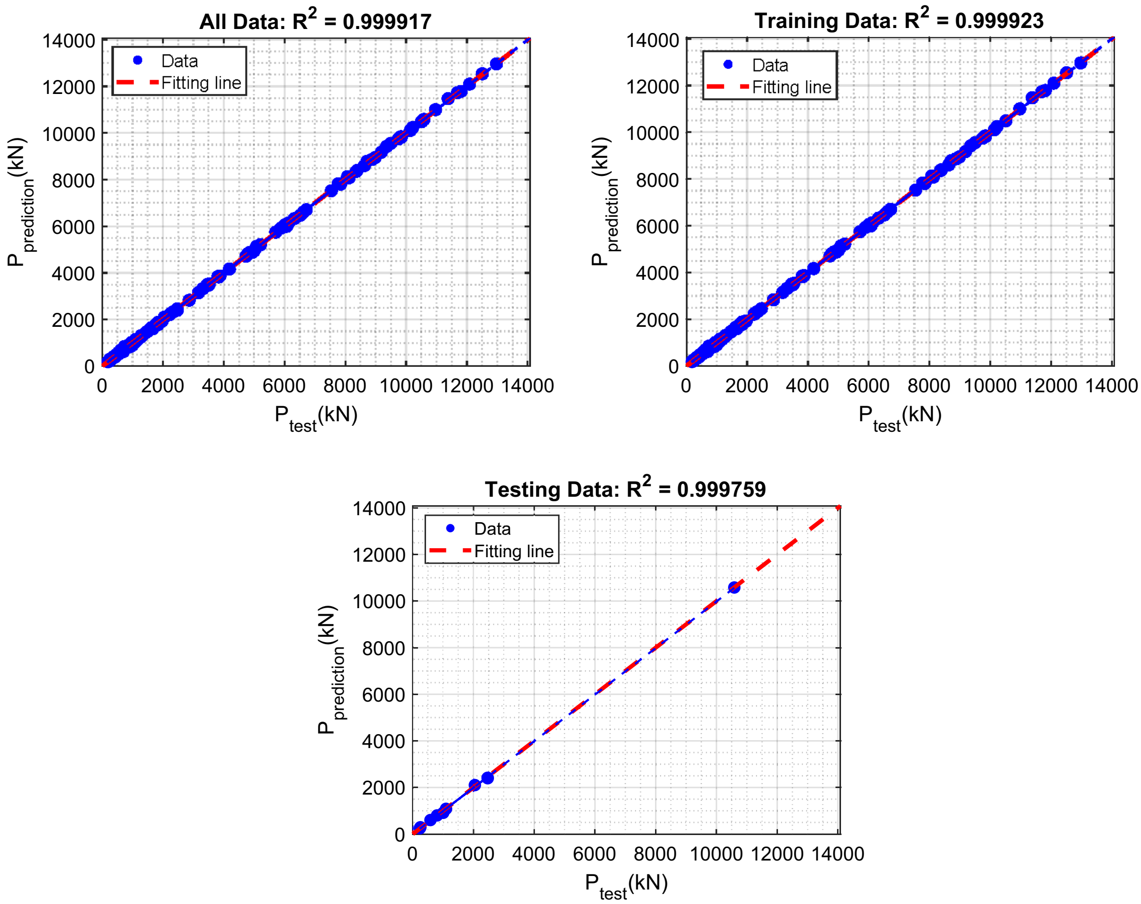

Fig. 6 Regression between the actual and the predicted value of the GBRT-01 model

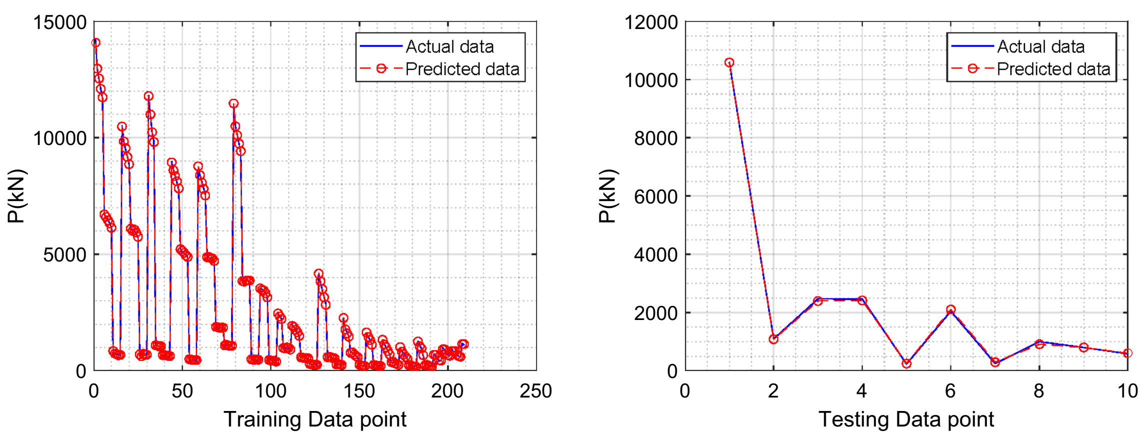

Fig. 7 Comparison between actual and predicted values

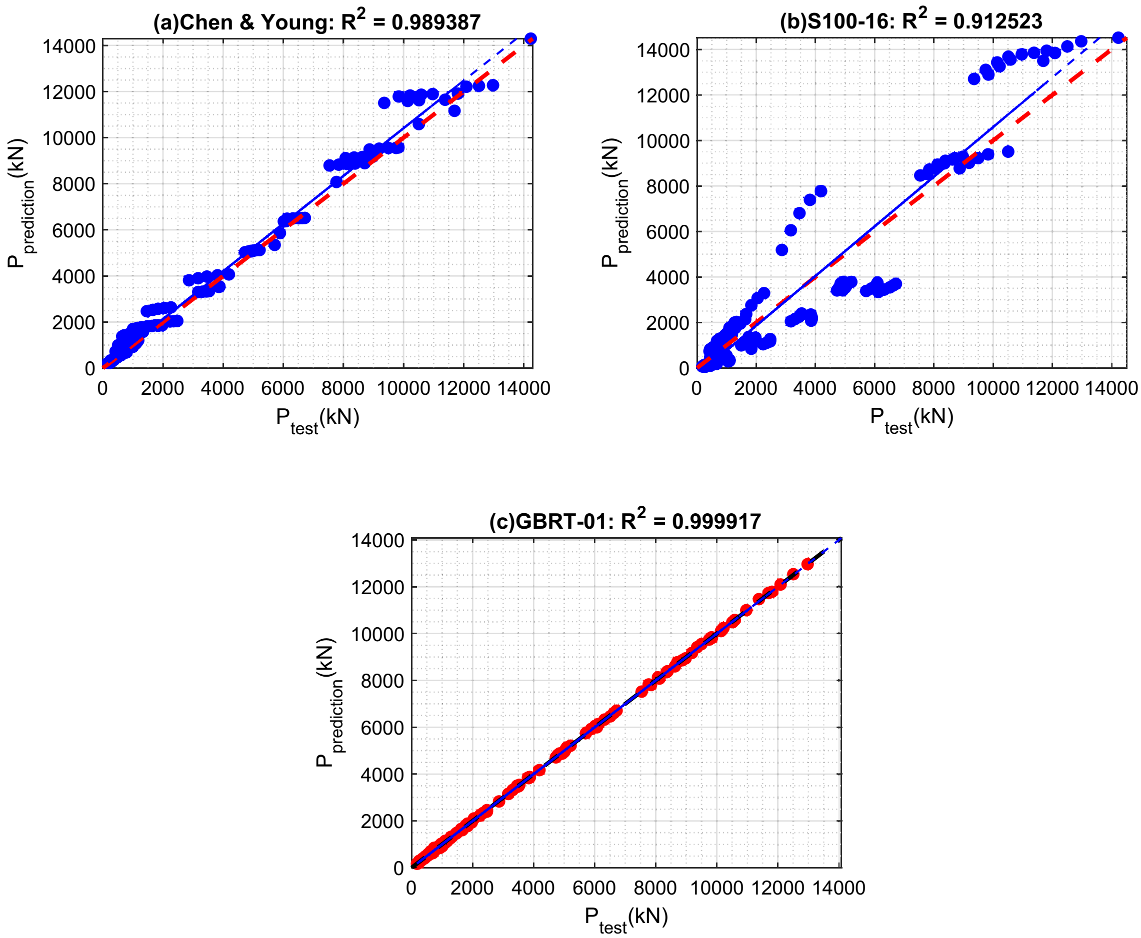

Fig. 8 Performance of Chen et al., S100-16, and GBRT-01 models

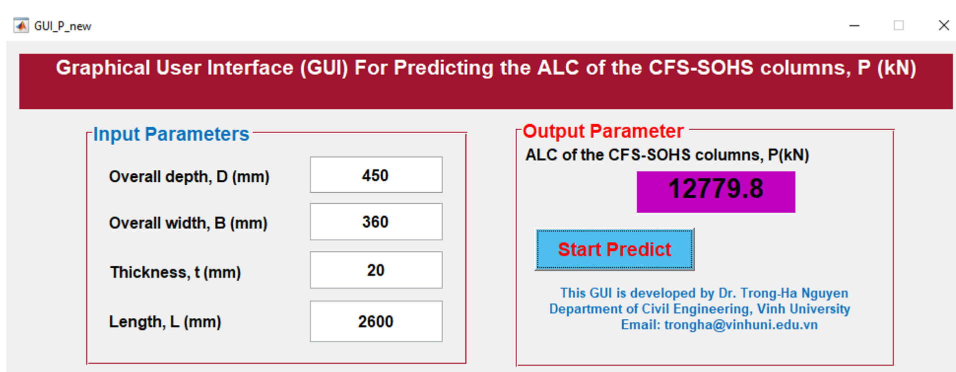

Fig. 9 The GUI for predicting the ALC of the CFS-SOHS columns

the two existing formulas. Can be seen that the GBRT-01 model has superior predictions for the ALC of the CFS-SOHS columns.

Figure 8 shows the regression between the actual and the predicted values of the GBRT-01 model, Chen et al. (Chen & Young, 2018b) and standard codes AISI-S100-16 (AISI-S100, 2016). As observed from Fig. 7a, b, it can be seen that the predicted values of Chen et al. and standard codes AISI-S100-16 have predicted values that are higher than the actual values (red line). Meanwhile, the predicted values of the GBRT-01 model and actual values almost completely coincide. Once again assertion that the GBRT-01 model has superior predictions for the ALC of the CFS-SOHS columns (Table 4).

Obviously, the GBRT-01 model has superior predictions for the ALC of the CFS-SOHS columns. However, it is not convenient for practicing design/research engineers to use. In this work, a practical graphical user interface (GUI) tool was built based on the regression model from results obtained GBRT-01 model, which is shown in Fig. 9, and it is provided freely.

Conclusions

This study developed the GBRT model for predicting the ALC of the CFS-SOHS columns. The GBRT-01 (training–testing set ratio of 0.95–0.05) has the most reliable prediction results based on the models ranking. A set of 219 data, in which the overall depth (D), the overall width (B), thickness (t), and column length (L) were considered as input parameters, while the ALC of the CFS-SOHS columns was the output parameter, was gathered to develop GBRT model. From the statistical metrics, the GBRT-01 model has superior predictions for the ALC of the CFS-SOHS columns than the two existing formulas. Specific conclusions of this research have been achieved as follows.

- The study has selected a training–testing appropriate ratio of 219 actual data with four input parameters and one output parameter to develop the GBRT model.
- The study applied the GBRT model for predicting the ALC of the CFS-SOHS columns. The statistical metrics from the GBRT model ($R^2 = 1.00, \mathrm{RMSE} = 41.3631, \mathrm{MAPE} = 1.3689,$ and $i20 - \mathrm{index} = 0.9966$) have been the best-predicting to the ALC of the CFS-SOHS column.
- A new graphical user interface (GUI) tool was built based on the regression model for practice design.

Supplementary Information The online version contains supplementary material available at https://doi.org/10.1007/s42107-023-00743-w.

Author contributions T-HN conceptualization, software, writing-original draft, writing-review & editing. D-DN methodology, formal analysis, writing–original draft, writing–review & editing, supervision.

Funding No funding was used in this study.

Data availability The data used to support the findings of this study are included in the article.

Declarations

Conflict of interest The authors declare that they have no known competing financial interests or personal relationships that could have appeared to influence the work reported in this paper.

References

AISI-S100. (2016). *North American Specification for the Design of Cold-Formed Steel Structural Members* (pp. 1–4). AISI.

Bakouregui, A. S., Mohamed, H. M., Yahia, A., & Benmokrane, B. (2021). Explainable extreme gradient boosting tree-based prediction of load-carrying capacity of FRP-RC columns. *Engineering Structures, 245*, 112836. https://doi.org/10.1016/j.engstruct.2021.112836

Chen, M.-T., & Young, B. (2018a). Cross-sectional behavior of cold-formed steel semi-oval hollow sections. *Engineering Structures, 177*, 318–330.

Chen, M.-T., & Young, B. (2018b). Experimental and numerical investigation on cold-formed steel semi-oval hollow section compression members. *Journal of Constructional Steel Research, 151*, 174–184. https://doi.org/10.1016/j.jcsr.2018.09.009

Dahiya, N., Saini, B., & Chalak, H. (2021). Gradient boosting-based regression modelling for estimating the time period of the irregular precast concrete structural system with cross bracing. *Journal of King Saud University-Engineering Sciences*. https://doi.org/10.1016/j.jksues.2021.08.004

Friedman, J. H. (2001). Greedy function approximation: a gradient boosting machine. *Annals of Statistics*. https://doi.org/10.1080/15567036.2019.1630521

Hao, X., Hu, X., Liu, T., Wang, C., & Wang, L. (2022). Estimating urban PM2. 5 concentration: An analysis on the nonlinear effects of explanatory variables based on gradient boosted regression tree. *Urban Climate, 44*, 101172. https://doi.org/10.1016/j.uclim.2022.101172

Kaveh, A. (2014). *Advances in metaheuristic algorithms for optimal design of structures*. Springer.

Kaveh, A., & Khavaninzadeh, N. (2023). Efficient training of two ANNs using four meta-heuristic algorithms for predicting the FRP strength. *Structures, 52*, 256–272.

Kaveh, A., & Servati, H. (2001). Design of double layer grids using backpropagation neural networks. *Computers & Structures, 79*(17), 1561–1568.

Manna, S., Biswas, S., Kundu, R., Rakshit, S., Gupta, P., & Barman, S. (2017). A statistical approach to predict flight delay using gradient boosted decision tree. In: *2017 International conference on computational intelligence in data science (ICCIDS)*

Naser, M., Thai, S., & Thai, H.-T. (2021). Evaluating structural response of concrete-filled steel tubular columns through machine learning. *Journal of Building Engineering, 34*, 101888. https://doi.org/10.1016/j.jobe.2020.101888

Nguyen, D.-D., Tran, V.-L., Ha, D.-H., Nguyen, V.-Q., & Lee, T.-H. (2021a). A machine learning-based formulation for predicting shear capacity of squat flanged RC walls. *Structures, 29*, 1734.

Nguyen, H. D., LaFave, J. M., Lee, Y.-J., & Shin, M. (2022a). Rapid seismic damage-state assessment of steel moment frames using machine learning. *Engineering Structures, 252*, 113737. https://doi.org/10.1016/j.engstruct.2021.113737

Nguyen, T.-H., Tran, N.-L., & Nguyen, D.-D. (2021b). Prediction of critical buckling load of web tapered I-section steel columns using artificial neural networks. *International Journal of Steel Structures, 21*(4), 1159–1181.

Nguyen, T.-H., Tran, N.-L., & Nguyen, D.-D. (2022b). Prediction of axial compression capacity of cold-formed steel oval hollow section columns using ANN and ANFIS models. *International Journal of Steel Structures, 22*(1), 1–26.

Nguyen, T.-H., Tran, N.-L., Phan, V.-T., & Nguyen, D.-D. (2023). Improving axial load-carrying capacity prediction of concrete columns reinforced with longitudinal FRP bars using hybrid GA-ANN model. *Asian Journal of Civil Engineering*. https://doi.org/10.1007/s42107-023-00695-1

Nieto, P. J. G., García-Gonzalo, E., Arbat, G., Duran-Ros, M., de Cartagena, F. R., & Puig-Bargues, J. (2018). Pressure drop modelling in sand filters in micro-irrigation using gradient boosted regression trees. *Biosystems Engineering, 171*, 41–51.

Prettenhofer, P., & Louppe, G. (2014). Gradient boosted regression trees in scikit-learn. PyData 2014.

Qi, C., Fourie, A., & Zhao, X. (2018). Back-analysis method for stope displacements using gradient-boosted regression tree and firefly algorithm. *Journal of Computing in Civil Engineering, 32*(5), 04018031. https://doi.org/10.1061/(ASCE)CP.1943-5487.0000779

Shatnawi, A., Alkassar, H. M., Al-Abdaly, N. M., Al-Hamdany, E. A., Bernardo, L. F. A., & Imran, H. (2022). Shear strength prediction of slender steel fiber reinforced concrete beams using a gradient boosting regression tree method. *Buildings, 12*(5), 550. https://doi.org/10.3390/buildings12050550

Tran, N.-L., Nguyen, T.-H., Phan, V.-T., & Nguyen, D.-D. (2021). A machine learning-based model for predicting atmospheric corrosion rate of carbon steel. *Advances in Materials Science and Engineering, 2021*, 1–25.

Tran, V.-L., & Kim, J.-K. (2022). JAYA-GBRT model for predicting the shear strength of RC slender beams without stirrups. *Steel and Composite Structures, 44*(5), 677–691. https://doi.org/10.12989/scs.2022.44.5.691

Tran, V.-L., & Kim, S.-E. (2020). Efficiency of three advanced data-driven models for predicting axial compression capacity of CFDST columns. *Thin-Walled Structures, 152*, 106744. https://doi.org/10.1016/j.tws.2020.106744

Tran, V.-L., Thai, D.-K., & Kim, S.-E. (2019). Application of ANN in predicting ACC of SCFST column. *Composite Structures, 228*, 111332. https://doi.org/10.1016/j.compstruct.2019.111332

Truong, V.-H., Vu, Q.-V., Thai, H.-T., & Ha, M.-H. (2020). A robust method for safety evaluation of steel trusses using Gradient Tree Boosting algorithm. *Advances in Engineering Software, 147*, 102825. https://doi.org/10.1016/j.advengsoft.2020.102825

Wang, F., & Song, G. (2020). Bolt-looseness detection by a new percussion-based method using multifractal analysis and gradient boosting decision tree. *Structural Health Monitoring, 19*(6), 2023–2032. https://doi.org/10.1177/1475921720912780

Zhu, J.-H., & Young, B. (2011). Cold-formed-steel oval hollow sections under axial compression. *Journal of Structural Engineering, 137*(7), 719–727. https://doi.org/10.1061/(ASCE)ST.1943-541X.0000337

Zhu, J.-H., & Young, B. (2012). Design of cold-formed steel oval hollow section columns. *Journal of Constructional Steel Research, 71*, 26–37. https://doi.org/10.1016/j.jcsr.2011.11.013

Zorlu, K., Gokceoglu, C., Ocakoglu, F., Nefeslioglu, H., & Acikalin, S. (2008). Prediction of uniaxial compressive strength of sandstones using petrography-based models. *Engineering Geology, 96*(3–4), 141–158. https://doi.org/10.1016/j.enggeo.2007.10.009